One-Dimensional Arrangement of Gold Nanoparticles by Electrospinning

Gyeong-Man Kim,*,† Andre Wutzler,† Hans-Joachim Radusch,† Goerg H. Michler,† Paul Simon,‡ Ralph A. Sperling,§ and Wolfgang J. Parak§

Department of Materials Science, Martin-Luther University, Halle-Wittenberg, D-06099 Halle/S, Germany, Center of Nanoscience, Ludwig-Maximilians University Munich, Schellingstrasse 4, D-80799 Munich, Germany, and Max Plank Institute for Chemical Physics of Solids, Nöthnitzer Strasse 40, D-01187 Dresden, Germany

Received April 18, 2005. Revised Manuscript Received July 12, 2005

The electrospinning technique was used successfully to fabricate one-dimensional arrays of Au nanoparticles within nanofibers in which the intrinsic nature of the semicrystalline polymer poly(ethylene oxide) (PEO) was employed as a template for the controlled nanoscale organization of nanoparticles. Differential scanning calorimetry (DSC), Fourier transform infrared spectroscopy, UV−visible spectroscopy, scanning electron microscopy, atomic force microscopy, and transmission electron microscopy (TEM) were performed to characterize the resulting electrospun fibers in comparison with pure PEO and PEO/Au nanocomposite before electrospinning. By choosing chloroform as the solvent in this work the observed electrospun fibers were about 400−650 nm in diameter and revealed a well-defined Gaussian distribution. Thermal analysis showed that the dodecanethiol-capped Au nanoparticles preferentially act as heterogeneous nucleating agents for PEO crystallization. Conformational changes occurred by incorporating Au nanoparticles as well as electrospinning. The most common helical structure of PEO was transformed into a trans zigzag planar structure due to the high extensional flow caused by electrospinning. As a striking result, fairly long and one-dimensional chainlike structures consisting of Au nanoparticles within the electrospun fibers were observed by TEM. The present findings demonstrate that the electrospinning process provides not only a fundamental understanding of the conformational changes upon process conditions, but also a straightforward and cost-effective technique to fabricate one-dimensional arrays of nanoparticles for future nanodevices with unique properties in various applications, such as biological sensors, single-electron transistors, photonic materials, etc.

1. Introduction

Metal nanoparticles,[1] which represent particularly attractive building blocks of individual atoms, hold promise for use as advanced materials with new electronic,[2] magnetic,[3] optical,[4] thermal,[5] and catalytic properties.[6] Compared with bulk materials, these unique properties mainly arise from the quantum-confinement effects and their enormous large specific surface areas. These nanoparticles provide a starting point for fabricating future nanodevices with unique electronic, optoelectronic, electrochemical, and electromechanical properties. Because the physical properties of these nanodevices are dominated by the formation of size-controlled nanoparticles, interparticle distances and their spatially ordered assemblies (superlattices) in predefined geometries, such as linear, two- and three-dimensional superstructures, have become the focus of intense research in recent years.[7] Among this line, two-dimensional (2D) and three-dimensional (3D) superlattices have been prepared by self-assembly,[8] the Langmuir−Blodgett method,[9] or electrophoretic deposition,[10] and their optical and electron transport properties have been intensely investigated. In contrast, one-dimensional (1D) arrays of nanoparticles still remain a great

* To whom correspondence should be addressed. E-mail: gyeong-man.kim@iw.uni-halle.de.
† Martin-Luther University Halle-Wittenberg.
‡ Max Plank Institute for Chemical Physics of Solids.
§ Ludwig-Maximilians University Munich.

(1) Pileni, M. P. *Metal Nanoparticles-Synthesis, Characterization, and Applications*; Feldheim, D. L., Colby, A. F., Jr., Eds.; Marcel Dekker: New York, 2002; Chapter 9. (b) Simon, U. *Metal clusters in Chemistry*; Braunstein, P., Oro, L. A., Raithby, P. R., Eds.; Wiley-VCH: Weinheim, 1999. (c) Schimd, G.; Bäumle, M.; Geerkens, M.; Heim, I.; Osemann, C.; Sawitowski, T. *Chem. Soc. Rev.* **1999**, *28*, 179. (d) Whetten, R. L.; Shafigullin, M. N.; Khoury, J. T.; Schaaff, T. G.; Vezmar, I.; Alvarez, M. M.; Wilkinson, A. *Acc. Chem. Res.* **1999**, *32*, 397.
(2) Kastner, M. A. *Phys. Today* **1993**, *46* (1), 24.
(3) (a) Sufi, R.; Kofinas, P. *J. Magn. Magn. Mater.* **2005**, *288*, 219. (b) Awschalom, D. D. *Science* **1996**, *271*, 937.
(4) (a) Alivisators, A. P. *Science* **1996**, *271*, 933. (b) Brus, L. *Appl. Phys. A* **1991**, *53*, 465.
(5) Negishi, N.; Takeuchi, K. *Thin Solid Films* **2001**, *392*, 249.
(6) Lewis, L. N. *Chem. Rev.* **1993**, *258*, 414.
(7) Wang, Z. L. *Adv. Mater.* **1998**, *10*, 13.
(8) (a) Lu, N.; Chen, X.; Molenda, D.; Naber, A.; Fuchs, H.; Talapin, D. V.; Weller, H.; Müller, J.; Lupton, J. M.; Feldmann, J.; Rogach, A.; Chi, L. *Nano Lett.* **2004**, *4*, 885. (b) Lopes, W. A.; Jaeger, H. M. *Nature* **2001**, *414*, 735.
(9) (a) Kim, F.; Kwan, J.; Akana, J.; Yang, P. *J. Am. Chem. Soc.* **2001**, *123*, 4360. (b) Martin, J. E.; Wilcoxon, J. P.; Odinek, J.; Provencio, P. *J. Phys. Chem. B* **2000**, *104*, 9475.
(10) (a) Li, Q.; Newberg, J. T.; Walter, E. C.; Hemminer, J. C.; Penner, R. M. *Nano Lett.* **2004**, *4*, 277. (b) Walter, E. C.; Zach, M. P.; Favier, F.; Murray, B.; Inazu, K.; Hemminger, J. C.; Penner, R. M. *Chemphyschem* **2003**, *4*, 131. (c) Limmer, S. J.; Seraji, S.; Tammy Y. W.; Chou, P.; Nguyen, C.; Cao, G. *Adv. Funct. Mater.* **2002**, *12*, 59. (d) Teranishi, T.; Hosoe, M.; Tanaka, T.; Miyake, M. *J. Phys. Chem. B* **1999**, *103*, 3818.

10.1021/cm0508120 CCC: $30.25
Published on Web 08/24/2005

challenge in nanotechnology[11] because it is quite difficult to organize metal nanoparticles in low symmetry. Successful realization of these structures in the future may provide a new tool to integrate these 1D nanostructures into functional devices and circuitry. Several approaches have been proposed to construct such structures by means of appropriate templates, such as DNA strands,[12] bacteria and viruses,[13] other linear polymers,[14] or lithographically patterned substrates.[15]

In the present work we demonstrate an alternative new approach based on the electrospinning (ES) technique for fabricating 1D arrangements of metal nanoparticle arrays within submicrometer polymer fibers. Recently, electrostatic fiber spinning, or "electrospinning", has received a growing attention because polymer fibers prepared by this technique achieve fiber diameters in the submicrometer range straightforwardly and cost-effectively.[16] To form such fibers using ES a polymer solution is forced through a capillary, forming a drop of polymer solution at the tip of capillary. Then a high voltage is applied between the tip and a grounded collection target. When the electric field strength overcomes the surface tension of the droplet, a polymer solution jet is initiated and accelerated toward the collection target. As the jet travels through the air, the solvent evaporates and a nonwoven polymeric fabric is formed on the target. This approach becomes particularly powerful when the ease and control offered by the nanofibers is combined with the electronic, magnetic, or photonic properties of inorganic components. To date, it has been well established that the ES process allows easily incorporating particles of materials, such as layered silicates,[17] carbon nanotubes,[18] and many others,[19] into the nanofibers.

The objectives of this research are 2-fold: One is to develop a single-step processing route for the production of synthetic fibers comprising a 1D arrangement of well-controlled metal nanoparticles. The other is to study the effect of electrospinning on the conformational changes of the resulting fibers with and without metal nanoparticles, which can provide fundamental insights into the nature of the electrospinning process. To achieve these objectives we employ semicrystalline polymer poly(ethylene oxide) (PEO) and its composites incorporated with gold nanoparticles. The choice of PEO is not only motivated by its wide variety of applications,[20] such as biomaterials including scaffolds,[21] drug delivery,[22] tissue engineering, wound healing,[23] and conductive fibers[24] for electrolytes in polymer batteries, but also by control of the dispersion of nanoparticles assisted by its intrinsic crystallinity that will contribute to fiber stability as well as responsibility for controlled dispersion of nanoparticles. Furthermore, the amphiphilic nature of PEO (soluble both in water and nonpolar solvents) and the strong dependence of local conformations on the used solvents make PEO an excellent model polymer for gaining a fundamental understanding of the conformational changes upon process conditions. The capability and feasibility of this technique demonstrates a promising alternative approach for the fabrication of polymer nanostructured composite fibers by controlling a set of experimental parameters.

2. Experimental Section

2.1. Materials. *Synthesis of Dodecanethiol-Capped Gold Nanoparticles.* Colloidal Au nanoparticles were synthesized according to standard protocols.[25] Briefly, 300 mg of hydrogen tetrachloroaurate ($HAuCl_4 \cdot 3H_2O$) dissolved in distilled water was added to 80 mL of a 50 μM tetraoctylammonium bromide ($[CH_3(CH_2)_7]_4NBr$) solution dissolved in toluene. Transfer of the metal salt to the toluene phase was clearly observed within a few seconds. An aqueous solution of 334 mg of sodium borohydride ($NaBH_4$) was added to the mixture while stirring, which immediately caused the reduction reaction. After 1 h the two phases were separated, and the toluene phase was washed with 0.01 M HCl, 0.01 M NaOH, and three times distilled H_2O. Afterward, a surfactant exchange procedure was carried out. A 10 mL amount of 1-dodecanethiol was added to the Au nanoparticles in toluene. The solution was heated to 65 °C and stirred for 2 h. During this process the mercapto groups of the dodecanethiol ($CH_3(CH_2)_{11}SH$) molecules bind to the surface of the Au nanocrystals, displacing the Br ions. Upon completion of the reaction, the final dodecanethiol-capped Au nanoparticles were precipitated twice with methanol and redissolved

(11) (a)Vidini, O.; Reuter, T.; Torma, V.; Meyer-Zaika, W.; Schmid, G. *J. Mater. Chem.* **2001**, *11*, 3188. (b) Thurn-Albrecht, T.; Schotter, J.; Kästle, G. A.; Emley, N.; Shibauch, T.; Krusin-Elbaum, L.; Guarini, K.; Black, C. T.; Tuominen, M. T.; Russell, T. P. *Science* **2000**, *290*, 2126.

(12) (a) Warner, M. G.; Hutchison, J. E. *Nature* **2003**, *2*, 272. (b) Mirkin, C. A. *Inorg. Mater.* **2000**, *39*, 2258. (c) Braun, E.; Eichen, Y.; Sivan, U.; Ben-Yoseph, G. *Nature* **1998**, *391*, 775. (c) Mirkin, C. A.; Letsinger, R. L.; Mucic, R. C.; Storhoff, J. J. *Nature* **1996**, *382*, 607.

(13) Hall, S. R.; Shenton, W.; Engelhardt, H.; Mann, S. *Chem. Phys. Chem.* **2001**, *3*, 184.

(14) Wyrna, D.; Beyer, N.; Schmid, G. *Nano Lett.* **2002**, *2*, 419.

(15) (a) Cui, Y.; Björk, M. T.; Liddle, J. A.; Sönnichsen, C.; Boussert, B.; Alivisatos, A. P. *Nano Lett.* **2004**, *4*, 1093. (b) Tsirlin, T.; Zhu, J.; Somorjai, G. A. *Top. Catal.* **2002**, *19*, 165.

(16) (a) Li, D.; Xia, Y. *Adv. Mater.* **2004**, *16*, 1151. (b) Sun, Z.; Zussman, E.; Yarin, A. L.; Wendorff, J. H.; Greiner, A. *Adv. Mater.* **2003**, *15*, 1929. (c) Shin, Y. M.; Hohman, M. M.; Brenner, M. P.; Rutledge, G. C. *Polymer* **2001**, *42*, 9955. (d) Deitzel, J. M.; Kleinmeyer, J.; Harris, D.; Beck, T. N. C. *Polymer* **2001**, *42*, 261. (e) Bognitzki, M.; Hou, H.; Ishaque, M.; Frese, T.; Hellwig, M.; Schwarte, C.; Schaper, A.; Wendorff, J. H.; Greiner, A. *Adv. Mater.* **2000**, *12*, 637. (f) Reneker, D. H.; Yarin, A. L.; Fong, H.; Koombhonges, S. *J. Appl. Phys.* **2000**, *87*, 4531. (g) Reneker, D. H.; Chun, I. *Nanotechnology* **1996**, *7*, 216. (h) Baumgarten, P. K. *J. Colloid Interface Sci.* **1971**, *36*, 71.

(17) (a) Fong, H.; Liu, W.; Wang, C.-S.; Vaia, R. A. *Polymer* **2002**, *43*, 775. (b) Kim, G.-M.; Lach, R.; Michler, G. H.; Chang, C. H. *Macromol. Rapid Commun.* **2005**, *26*, 728.

(18) (a) Dror, Y.; Salalha, W.; Khalfin, R. L.; Cohen, Y.; Yarin, A. L.; Zussman, E. *Langmuir* **2003**, *19*, 7012. (b) Salalha, W.; Dror, Y.; Khalfin, R. L.; Cohen, Y.; Yarin, A. L.; Zussman, E. *Langmuir* **2004**, *20*, *9852*. (c) Kim, G.-M.; Michler, G. H.; Pötschke, P. *Polymer*, **2005**, *46*, 7346.

(19) Wang, M.; Singh, H.; Hatton, T. A.; Rutledge, G. C. *Polymer* **2004**, *45*, 5505.

(20) Christie, A. M.; Lilley, S. J.; Staunton, E.; Yuri, G.; Andreev, Y. G.; Bruce, P. G. *Nature* **2005**, *433*, 50.

(21) Duan, B.; Dong, C.; Yuan, X.; Yao, K. *J. Biomater. Sci., Polym. Ed.* **2004**, *15*, 797.

(22) (a) Zeng, J.; Xu, X.; Chen, X.; Liang, Q.; Bian, X.; Yang, L.; Jing, X. *J. Controlled Release* **2003**, *92*, 227. (b) Kenaway, E. R.; Bowling, G. L.; Wnek, G. E. *J. Controlled Release* **2002**, *81*, 57.

(23) Hirano, S.; Zhang, M.; Nakagawa, M.; Miyata, T. *Biomaterials* **2000**, *21*, 997.

(24) (a) Qin, X. Y.; Wan, Y. Q.; He, J. H.; Zhang, J.; Yu, J. Y.; Wang, S. Y. *Polymer* **2004**, *45*, 6409. (b) MacDiarmid, A. G.; Ones, W. E.; Norris, I. D., Jr.; Gao, J.; Johnson, A. T.; Pinto, N. *J. Synth. Met.* **2001**, *119*, 27.

(25) (a) Gittins, D. I.; Caruso, F. *Angew. Chem., Int. Ed.* **2001**, *40*, 3001. (b) Templeton, A. C.; Wuelfing, W. P.; Murray, R. W. *Acc. Chem. Res.* **2000**, *33*, 27. (c) Kiely, C. J.; Fink, J.; Zheng, J. G.; Brust, M.; Bethell, D.; Schiffrin, D. J. *Adv. Mater.* **2000**, *12*, 640. (d) Fink, J.; Kiely, C. J.; Bethell, D.; Schiffrin, D. J. *Chem. Mater.* **1998**, *10*, 922. (e) Leff, D. V.; O'Hara, P. C.; Heath, J. R.; Gelbart, W. M. *J. Phys. Chem.* **1995**, *99*, 7036−7041.

in chloroform ($CHCl_3$) to prepare the PEO nanocomposites and electrospinning of them. The overall concentration of the resulting Au nanoparticle solution was 20 μM.

PEO and PEO/Au Nanocomposites. The semicrystalline polymer poly(ethylene oxide) (PEO, M_w = 600 000 g/mol) was purchased from Aldrich Chemical Co. Inc. and used as received without further purification. PEO/Au composite films were prepared by a solution-cast technique using chloroform as the solvent at room temperature. First, PEO powder was dissolved in chloroform to make a 2 wt % solution and then mixed with a 1 wt % solution of dodecanethiol-capped Au dissolved in chloroform. The mixture was vigorously stirred with a magnetic stir bar for at least 24 h at room temperature and casted onto glass dishes, and subsequently the solvent was evaporated slowly in air at room temperature for 2 days. To ensure complete solvent removal, the final nanocomposites (NCs) were annealed at 55 °C for 12 h in a vacuum oven at 0.5 Torr.

2.2. Methods. *Electrospinning Process.* To obtain electrospinnable solutions, pure PEO and its NCs were dissolved in chloroform to prepare a 2 wt % solution. The solution was vigorously stirred with a magnetic stir bar for at least 24 h at room temperature, which was followed by sonication for 30 min to ensure a homogeneous solution. ES was carried out under ambient temperature in a vertical spinning configuration using a 1 mm i.d. flat-end needle with a 5 cm working distance. The applied voltages were in the range from 3 to 20 kV, driven by a high-voltage power supply (Knürr-Heizinger PNC, Germany). The electrospun fibers were collected either on Cu grids or slide glasses. The samples were annealed at 55 °C for 12 h and cooled to room temperature under vacuum (0.5 Torr).

Investigation of Fiber Morphology: Electron Microscopy and Atomic Force Microscopy (AFM). To characterize the size of the Au nanoparticles and their spatial dispersion within the electrospun fibers, the PEO fibers were directly electrospun on Cu grids covered with an ultrathin carbon layer and investigated by conventional transmission electron microscopy (TEM) (JEOL 200CX operated at 200 kV) as well as by high-resolution TEM (Philips CM200 FEG\ST Lorentz electron microscope with a field emission gun and at an acceleration voltage of 200 kV). For the analysis of the diameter of the electrospun fibers and their distribution the electrospun fibers collected on the slide glasses were investigated by field emission gun-environmental scanning electron microscopy (FEG-ESEM, Philips ESEM XL 30 FEG). To study the morphology of the PEO crystals upon the electrospinning process, AFM (Digital Instrument, NanoScope IIIa) with commercially available Si_3N_4 cantilevers was employed. The tapping mode of AFM was selected to obtain both height and phase images. The scanner was calibrated with a standard grid in both lateral size and height.

Differential Scanning Calorimetry (DSC). DSC measurements were conducted to measure the melting and crystallization behavior with a Mettler-Toledo DSC 820 under a nitrogen atmosphere. The samples were sealed in aluminum pans and heated and cooled in the temperature range 25−100 °C in the DSC instrument with a rate of 10 °C/min. The weight of each sample was approximately 0.5 mg. The DSC temperature and heat flow values were calibrated with indium as the standard. The degree of crystallinity, X_c, was calculated from the endothermic area by the following equation

$$X_C = \Delta H_{fus}/\Delta H_{fus}^{\ 0}$$

where $\Delta H_{fus}^{\ 0}$, the heat of fusion of 100% crystalline PEO (M_w = 600 000 g/mol), was taken as 190 J/g from the literature[26] and ΔH_{fus} is the heat of fusion for the sample obtained from the endothermic area of the melting trace.

Optical Measurements. An FTIR spectrometer (FTIR Spectrometer S2000, Perkin-Elmer) equipped with a fixed 100 μm diameter aperture and a mercury−cadmium−telluride (MCT) detector was used to analyze the absorbance in the wavenumber range of 400−4000 cm^{-1} with a resolution of 2 cm^{-1}, monitoring the conformational changes caused by introduction of Au nanoparticles into PEO and the electrospinning process. To obtain a spectrum of pure amorphous PEO, PEO powder (about 1 mg) was melted on the surface of a diamond single attenuated total reflectance (ATR) cell (Golden Gate) at 100 °C. To characterize the PEO molecular orientation within electrospun fibers with and without Au nanoparticles, polarized FTIR measurements using a Zn−Se wire grid infrared polarizer were performed on two or three selected areas in a single electrospun fiber. At each area the parallel and perpendicular spectra relative to the fiber axis were recorded. UV−visible absorption spectra of colloidal Au nanoparticles using a 1 cm quartz cuvette were measured on a Perkin-Elmer Lambda 3B spectrophotometer.

3. Results and Discussion

3.1. Fiber Morphology. Figure 1 shows FEM−SEM micrographs of the electrospun fibers from pure PEO and PEO/Au NC and their diameter distribution. In both cases the fibers, which were electrospun under the optimized ES conditions used (5 cm working distance, 2 wt % solution in chloroform), are uniform without any evidence of "beads on a string" morphology. This observation is consistent with the results by R. Jaeger et al.[27] Pure PEO fibers exhibit a smooth surface, whereas the PEO/Au nanocomposite fibers are rather rough. The diameter of the electrospun fibers in both cases resembles a Gaussian distribution. The average diameter lies at 500 nm in pure PEO fibers and shifts to 550 nm in the PEO/Au nanocomposite fibers with broader distribution.

The dispersion of Au nanoparticles within the electrospun fibers was examined by TEM. A striking feature observed on all electrospun fibers containing Au nanoparticles is the formation of extended and closely packed linear nanoparticle chains along the fiber direction, as shown in Figure 2. Within the electrospun fibers of PEO/Au nanocomposite fairly long, closely spaced nanoparticles and a high degree of linearity were observed. All of the linear assemblies observed by TEM display an extended chainlike "necklace" structure. The length of these assemblies appears to be nearly several hundreds micrometers, which is not surprising because ES can straightforwardly produce long continuous fibers up to millimeters in length.

Hereby, the intrinsic semicrystalline feature of PEO may play a crucial role to direct the particular arrangements of nanoparticles during the electrospinning process. In addition, gold nanoparticles were organized with an almost regular spacing due to the dodecanethiol molecules on the particle surface (Figure 3a). Figure 3b shows a HR-TEM micrograph of an individual gold nanoparticle and its fast Fourier transform (FFT) image (inset). The average particle size was about 4 nm in diameter. The HR-TEM image clearly shows crystal lattice fringes of 0.24 nm, corresponding to the (111)

(26) (a) Booth, C.; Devoy, C. J.; Gee, G. *Polymer* **1971**, *12*, 327. (b) Marco, C.; Fatou, J. G.; Gomez, M. A.; Tanaka, H.; Tonelli, A. E. *Macromolecules* **1990**, *23*, 2183.

(27) Jaeger, R.; Bergshoef, M.; Batle, C. M.; Schönherr, H.; Vancso, G. J. *Macromol. Symp.* **1998**, *127*, 141.

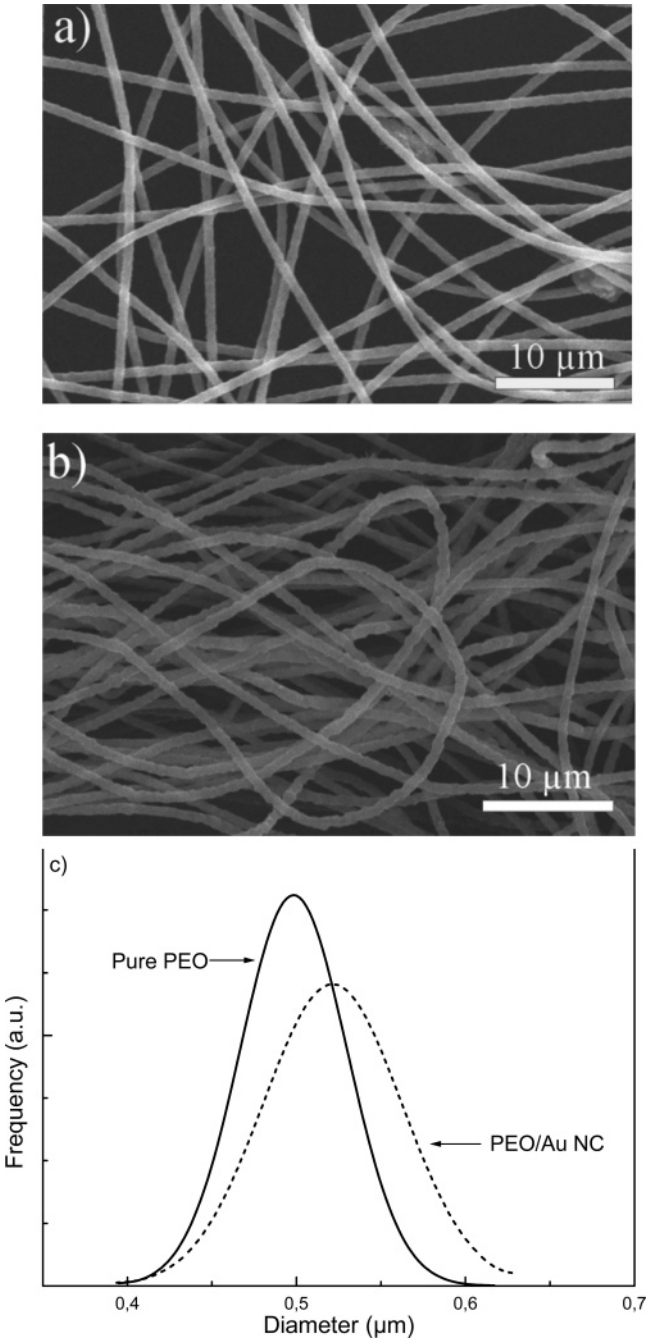

Figure 1. SEM micrographs: (a) electrospun PEO fibers, (b) electrospun PEO/Au NC fibers, and (c) their diameter distributions.

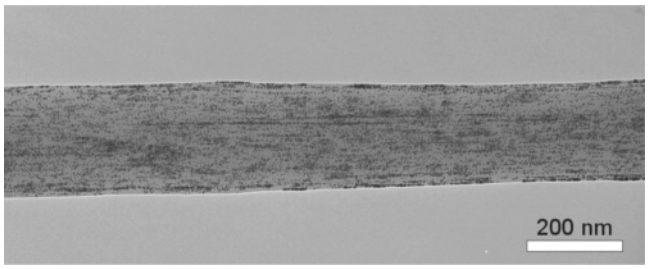

Figure 2. TEM micrograph of 1D chainlike arrays of Au nanoparticles.

lattice planes of fcc.[28] It is also noticed here that other areas in the electrospun fibers provide evidence that some chains

(28) Andres, R. P.; Bielefeld, J. D.; Henderson, J. I.; Janes, D. B.; Kolagunta, V. R.; Kubiak, C. P.; Mahnoney, W.; Osifchin, R. G. *Science* **1996**, *273*, 1690.

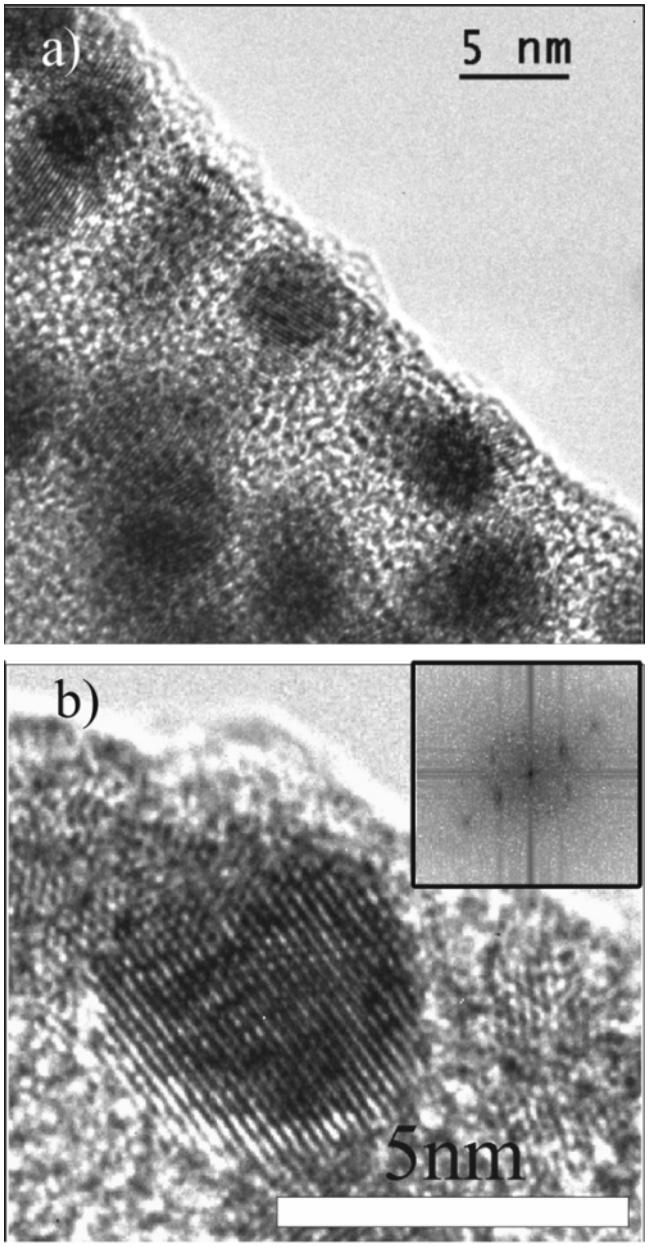

Figure 3. HR-TEM images: (a) close-up image from an area near the surface of the fibers and (b) image of an individual Au nanoparticle and its FFT image shown as inset.

are assembled into 3D bundles, which may be caused by overlapping of the 1D chains of Au nanoparticles.

The UV−vis absorption spectrum shows an absorption band with a peak maximum at 518 nm which arises from surface plasmon absorption of Au nanoparticles (Figure 4) with an assumed optical extinction coefficient of 8.7×10^6 M^{-1} cm^{-1}. The electrospun fibers, both with and without Au nanoparticles, revealed a well-defined birefringence in a polarized optical microscope (data not shown here). This indicates that the PEO molecules may be aligned along the fiber axis due to the elongational flow during electrospinning. Figure 5 shows AFM surface images of electrospun fibers exhibiting a perpendicular arrangement of PEO lamellae to the fiber axis, where a and b are taken from pure PEO and PEO/Au nanocomposite, respectively. As expected for

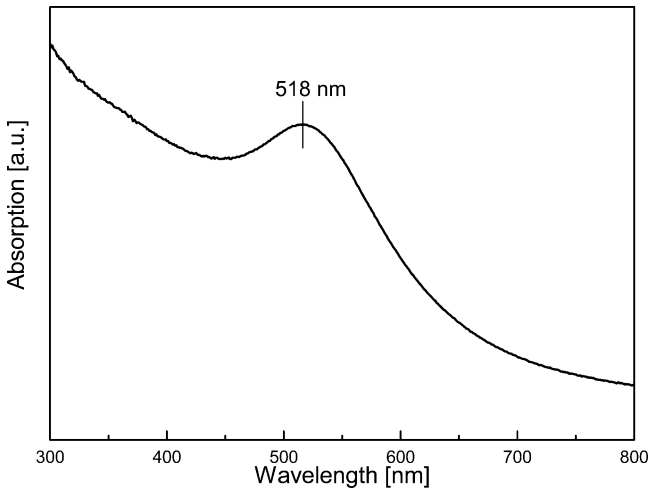

Figure 4. UV−vis spectrum of dodecanethiol-capped Au nanoparticle.

molecule chains aligned parallel to the fiber direction, the resulting lamellae should be perpendicular to the fiber axis, i.e., a so-called shish-kebab structure.[18a] Figure 5 clearly confirms this argument. AFM shows that the lamellae in the PEO electrospun fibers are thicker and less perpendicularly organized compared to those of the PEO/Au nanocomposite fibers. The lamellar thickness and their long period are 25 and 36 nm in pure PEO electrospun fibers, whereas they are 18 and 30 nm in PEO/Au nanocomposite fibers. These results are consistent with those from DSC and FTIR measurements as will be discussed later. Such a parallel arrangement of nanoparticles with respect to a host polymer with distinct chainlike nanowires should be useful to fabricate future nanodevices.

3.2. Differential Scanning Calorimetry (DSC). To investigate the thermal behavior, such as melting, crystallization, and formation of a crystalline structure, we performed DSC measurements. The most interesting feature in the DSC traces in this study is that all samples show a single endo- and exothermal peak (Figure 6). The endothermic peaks during the heating stage, which are centered at 63−66 °C, are shown in Figure 6a. This is attributed to the melting of the crystalline PEO phase.[29] From the enthalpy associated with the melting endotherm the crystallinity of samples studied was calculated using the value 190 J/g as the enthalpy of fusion of 100% crystalline PEO (M_w = 600 000 g/mol) from the literature.[23]

As reported in Table 1, after incorporation of Au nanoparticles as well as after the electrospinning procedure the melting temperature shifts moderately to higher values compared with pure PEO. However, the melting enthalpy—degree of crystallinity—increases drastically after incorporation of Au nanoparticles; the most significant change occurs in electrospun fibers of PEO/Au NC. These results indicate that there are some interactions between PEO and Au nanoparticles. Furthermore, the electrospinning procedure favors increasing both the melting temperature and crystallinity. From these results it is concluded that the nanoparticles preferentially serve as heterogeneous nucleation sites for PEO crystallization. In addition, the electrospinning procedure causes breakage of the long chains of the crystalline complex into small parts. As a consequence, the lamellae in PEO/Au NC fibers appear to be thinner compared to pure PEO fibers (see Figure 5). Figure 6b shows the exotherms upon cooling the melt. Although the exothermic peak of pure PEO is unaffected by the presence of Au nanoparticle in the PEO matrix, it is significantly shifted to higher temperatures upon electrospinning, corresponding to promoted rapid crystallization. This may be caused by confined crystallization through the dimensional reduction of the material during the electrospinning process.

It is interesting to note from the DSC diagrams that the crystallization and melting peak in both systems containing Au nanoparticles appear sharper and narrower before and after electrospinning compared to those without Au nanoparticles. This result may be at least in part attributed to the higher thermal conductivity of Au nano-

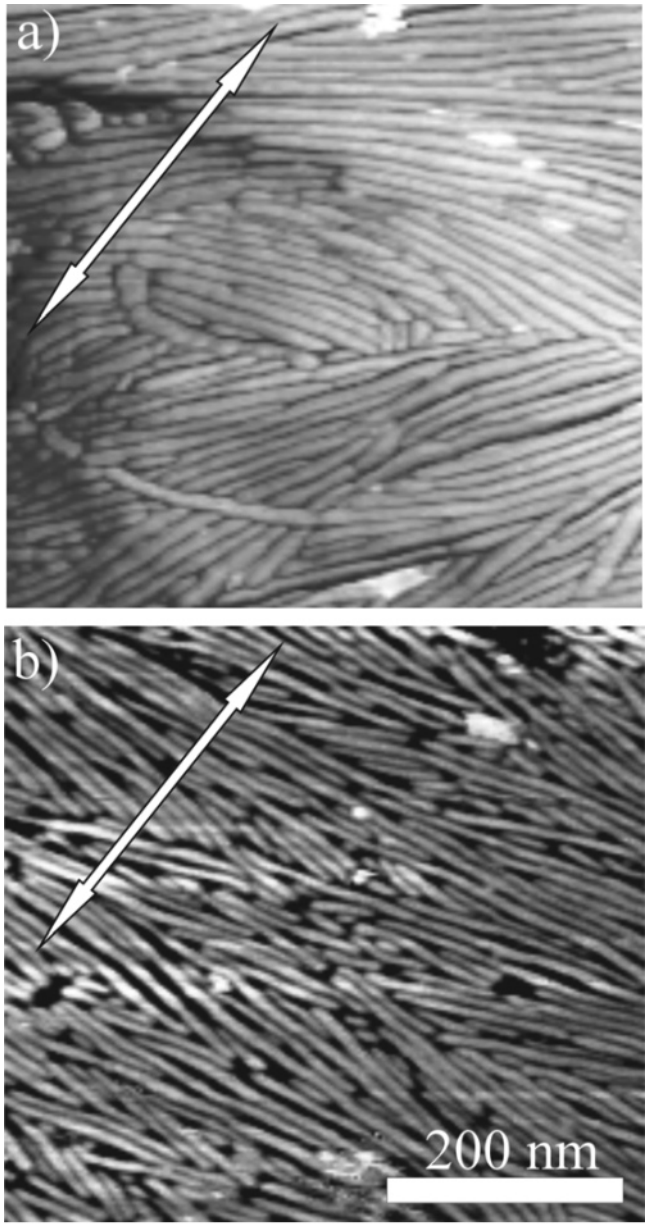

Figure 5. AFM images showing the surface morphology: (a) electrospun PEO fibers and (b) electrospun PEO/Au NC fibers (the arrow indicates the fiber direction).

(29) Buckley, C. P.; Kovacs, A. J. *Structure of Crystalline Polymers*; Hall, I. H., Ed.; Elsevier Applied Science: London, 1984.

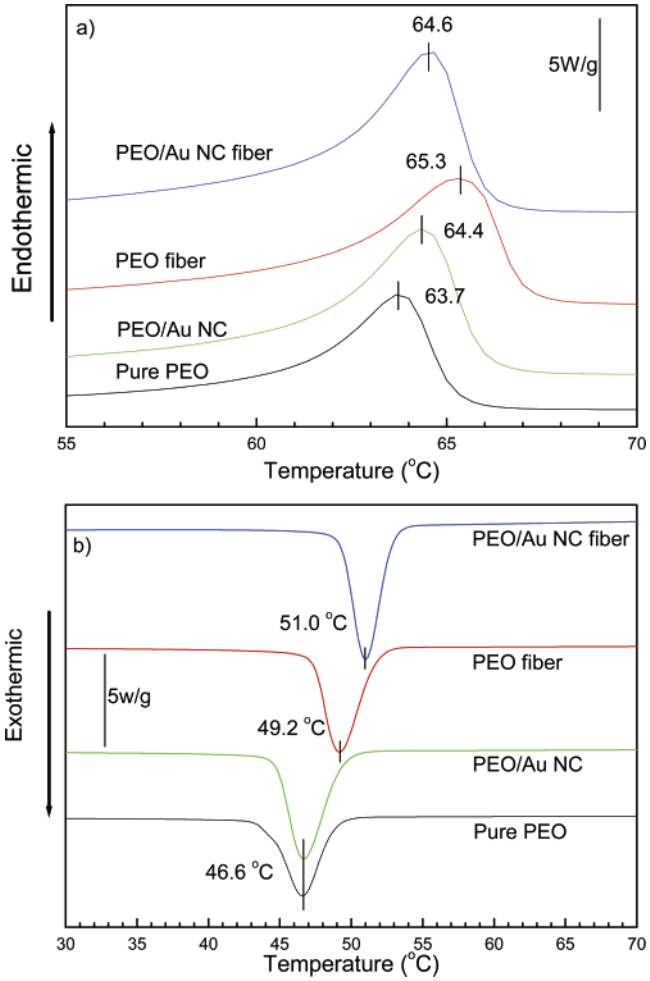

Figure 6. DSC diagrams for pure PEO, PEO/Au NC, electrospun PEO fibers, and electrospun PEO/Au NC fibers: (a) endothermic and (b) exothermic traces.

Table 1: Melting and Crystallization Temperatures, Melting Enthalpies, and Calculated Crystallinities

	T_m (°C)	T_c (°C)	ΔH_m (J/g)	crystallinity (%)
pure PEO	63.7	46.5	83.22	44
PEO/Au NC	64.4	46.5	113.57	60
PEO fiber	65.3	49	110.51	58
PEO/Au NC fiber	64.6	51	117.33	62

particles compared to that of PEO as heat will be more diversely distributed in the samples containing the Au nanoparticles. Thus, Au nanoparticles provide a high degree of supercooling during the crystallization processes while electrospinning, which leads to rapid formation of heterogeneous crystallization nuclei. Consequently, narrow crystallization and melting peak are associated with a narrow crystallite size distribution in the PEO/Au NC electrospun fibers compared to PEO fibers and in the PEO/Au nanocomposite compared to pure PEO. These results are also consistent with AFM results.

3.3. FTIR. Although DSC is informative for the thermal behavior, it does not give any information about the nature of the conformational changes upon introduction of Au nanoparticles and the electrospinning procedure. To characterize the conformational changes we conducted FTIR measurements. Figure 7a shows a FTIR spectrum (600−4000 cm^{-1}) from dodecanethiol-capped Au nanoparticles. The band positions and their assignments are listed in Table 2.[30]

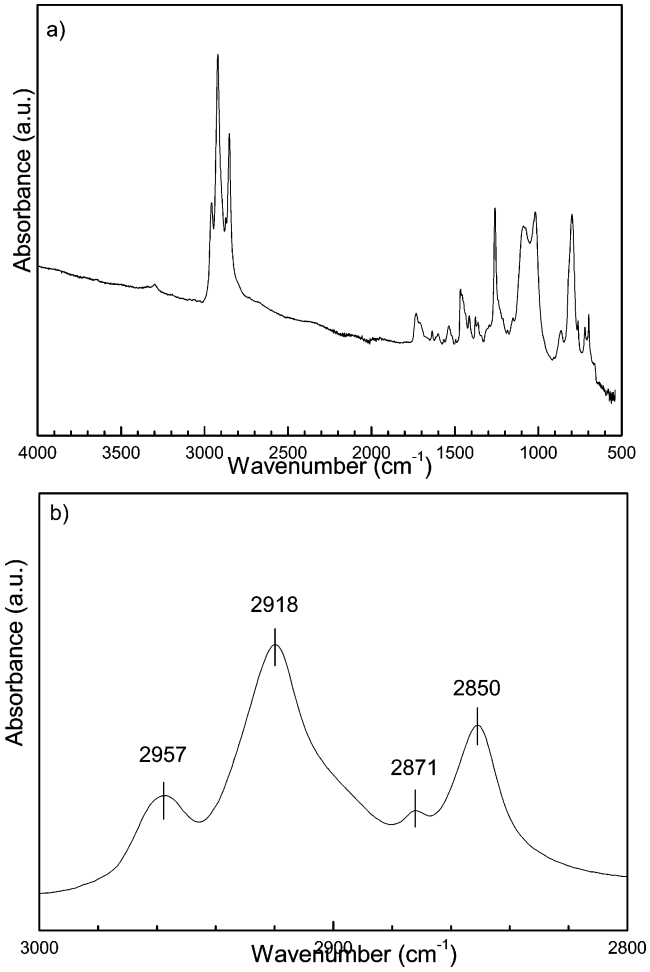

Figure 7. FTIR spectrum for dodecanethiol-capped Au nanoparticles: (a) whole range studied and (b) close-up spectrum from 2800 to 3000 cm^{-1}.

Table 2: FTIR Data for Dodecanethiol-Capped Au Nanoparticles and Their Assignments

absorbance peak (cm^{-1})	assignment
2957	CH_3 asymmetric stretching
2918	CH_2 asymmetric stretching
2871	CH_3 symmetric stretching
2850	CH_2 symmetric stretching
1466	CH_2 scissoring
1413	CH_2 scissoring adjacent to the Au-S bond
1377	CH_3 symmetric bending[40]

The very weak SH stretching vibration mode is usually observed at 2560 cm^{-1}.[31] However, this is not visible for dodecanethiol-capped Au nanoparticles, indicating that bonding of the dodecanethiol ligands to the Au surface takes place via Au−S bonds. As a consequence, a new band appearing at 1413 cm^{-1} can be assigned to a scissoring vibration mode of the CH_2 group adjacent to the Au−S bond. These results are consistent with those reported by others.[32] The bands at 1466 and 1377 cm^{-1} arise from the asymmetric and sym-

(30) (a) Manna, A.; Imae, T.; Yogo, T.; Aoi, K.; Okazaki, M. *J. Colloid Interface Sci*. **2002**, *256*, 297. (b) Porter, M. D.; Bright, T. B.; Allara, D. L.; Chidsey, C. E. D. A. *Am. Chem. Soc*. **1987**, *109*, 3559.
(31) (a) Laibinis, P. E.; Whitesides, G. M.; Allara, D. L.; Tao, Y.-T.; Parikh, A. N.; Nuzzo, R. G. *J. Am. Chem. Soc*. **1991**, *113*, 7152. (b) Hayashi, M.; Shiro, Y.; Murata, H. *Bull. Chem. Soc. Jpn.* **1966**, *39*, 112.
(32) (a) Hasan, M.; Bethell, D.; Brust, M. *J. Am. Chem. Soc*. **2002**, *124*, 1132. (b) Hostetler, J. M.; Stokes, J. J.; Murray, R. W. *Langmuir* **1996**, *12*, 3604. (c) Smith, E. L.; Porter, M. D. *J. Phys. Chem*. **1993**, *97*, 8032.

metric bending vibration of the methyl group (CH_3), respectively. They can be attributed to the assignments caused by the capping effect. Common vibrational features due to the presence of thiols are represented in the range 2800−3000 cm^{-1} (Figure 7b). The fact that in the spectrum of nanoparticles the CH_2 asymmetric and symmetric stretching bands are observed at 2918 and 2850 cm^{-1} suggests that the alkyl chains of dodecanethiol are extended with a trans zigzag conformation onto the gold particle surface.[33] The higher wavenumbers of CH_3 stretching modes are observed at 2957 and 2855 cm^{-1}. This indicates that the thiol molecules are not leached out after washing of the particles during the synthesis of Au nanoparticles.

PEO ($[-(CH_2)_2-O-]_n$) is a semicrystalline polymer whose the crystal structure is well known from X-ray scattering, neutron diffraction, and IR absorption, usually in a monoclinic phase.[34] The polymer chains consist of seven $O-CH_2-CH_2$ repeat units, which have an extended structure of 19.3 Å length over two turns of the helix, i.e., 7/2 helical conformation. Internal rotations around the $O-CH_2$, CH_2-CH_2, and CH_2-O bonds yield the trans (T), gauche (G), and trans (T) form, respectively, and the resulting helical conformation, TGT. This helical conformation is thermodynamically stable and therefore most commonly observed.[32] It has been well established that PEO is preferentially transformed into a planar zigzag conformation (TTT) under tension[35] or when water is added, exhibiting a triclinic crystal structure with an identical chain length of 7.12 Å.[31,35,36]

To characterize the conformational change in the PEO matrix upon incorporation of Au nanoparticles and electrospinning, FTIR measurements were first performed on the pure PEO. Figure 8 illustrates the vibrational bands of pure PEO from powder and its melt at 120 °C.

The absorption peaks, their assignments, and the type of dominant conformations are summarized in Table 2. The vibrational bands of the crystalline PEO are observed as follows:[31−37] The bands at 1467 and 1455 cm^{-1} correspond to CH_2 bending, the bands at 1411 and 1341 cm^{-1} to a CH_2 wagging motion, the band 1358 cm^{-1} to the mixed motion of CH_2 wagging and CC stretching, the 1278, 1240, and 1235 cm^{-1} bands to CH_2 twisting, the band at 1144 cm^{-1} to the mixed motion of CC and COC stretching, the 1093 cm^{-1} band to COC stretching, the band at 1060 cm^{-1} to the mixed motion of CH_2 rocking and COC stretching, the bands at 961 and 947 cm^{-1} to CH_2 rocking, and the 842 cm^{-1} band to CH_2 bending. For comparison, the FTIR spectrum of purely amorphous PEO was obtained from the molten state of PEO. The doublet bands at 1341, 1358, 943, and 964 cm^{-1} which were visible for the crystalline PEO phase disappear completely in the molten state and turn into singlets at 1457, 1350, 1292, 1250, 939, and 850 cm^{-1}. These singlet bands are attributed to the vibrational modes of conformationally irregular PEO chains (purely amorphous).[31a] In the spectrum of amorphous PEO we do not find any indication of either helical or trans planar zigzag conformations, as will be discussed later.

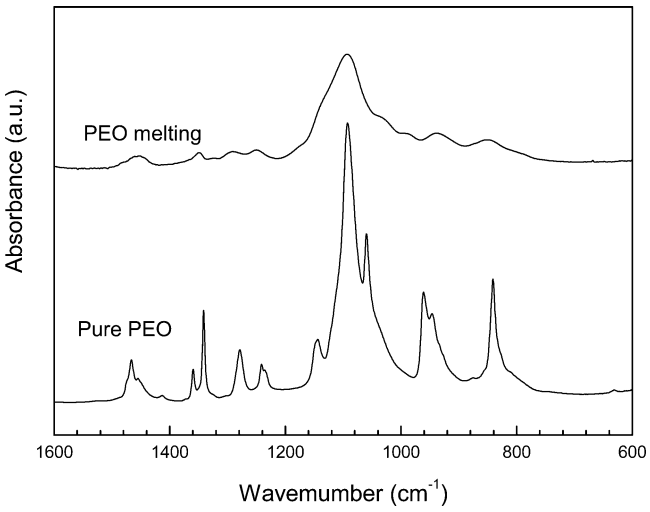

Figure 8. FTIR spectra taken from PEO powder (crystalline) and its melt (amorphous).

The FTIR spectra of all different samples investigated here are shown in Figure 9. Except for variations in the intensity of these bands, all peaks remain at the same location, i.e., no significant shifts are visible. In addition, the spectra obtained at room temperature do not contain any vibrational bands of amorphous PEO. These results strongly suggest that all materials at room temperature are in the semicrystalline state. It is most interesting to note here that FTIR spectra recorded in the present work indicate a coexistence of at least two different molecular chain conformations. The most characteristic bands of the thermodynamically stable helical structure are located at 1358, 1278, 1235, 1060, 947, and 842 cm^{-1} and those of the trans planar conformation at 1341, 1240, and 961 cm^{-1}. For simplicity, here we denote the helical and trans planar structures as H and T, respectively. It can be clearly seen in Figure 9 that the band at 1060 cm^{-1}, which is attributed to the H structure of PEO, almost disappears in the electrospun fibers of both systems with and without Au nanoparticles. This indicates that the high extensional force caused by the electrospinning process causes the PEO chains to be preferentially more aligned in the fiber direction, thus forming the T rather than the H conformation. This is consistent with the results observed from PEO under simple tension.

To obtain a deeper insight of the H and T population, we selectively considered the ratio between 1358 and 1341 cm^{-1} (arrows a and b of Figure 9), respectively.[38] Other strong lines more or less correspond to the two conformational modifications and, therefore, are not taken into account here. As listed in Table 4, the T/H absorbance ratio (i.e., A_{1341}/

(33) (a) Nuzzo, R. G.; Dubios, L. H.; Allara, D. L. *J. Am. Chem. Soc.* **1990**, *112*, 558. (b) Proter, M. D.; Bright, T. B.; Allara, D. L.; Chidsey, C. E. D. *J. Am. Chem. Soc*. **1987**, *109*, 3559.

(34) (a) Dissanayake, M. A. K. L.; Frech, R. *Macromolecules* **1995**, *28*, 5312. (b) Shimomura, M.; Tanabe, Y.; Watanabe, Y.; Kobayashi, M. *Polymer* **1990**, *31*, 1411. (c) Takahashi, Y.; Tadokoro, H. *Macromolecules* **1973**, *6*, 672. (d) Tadokoro, H.; Chatani, Y.; Yoshihara, T.; Tahara, S.; Murahashi, S. *Makromol. Chem*. **1964**, *73*, 109.

(35) (a) Tai, K.; Tadokoro, H. *Macromolecules* **1974**, *7*, 507. (b) Takahashi, Y.; Sumita, I.; Tadokoro, H. *J. Polym. Sci., Polym. Phys. Ed*. **1973**, *11*, 2113.

(36) Rao, G. R.; Castiglioni, C.; Gussoni, M.; Zerbi, G.; Martuscelli, E. *Polymer* **1986**, *26*, 811.

(37) (a) Marentrtte, J. M.; Brown, G. R. *Polymer* **1998**, *39*, 1405.

(38) Shieh, Y.-T.; Liu, K.-H. *J. Polym. Sci., Part B: Polym. Phys.* **2004**, *42*, 2479.

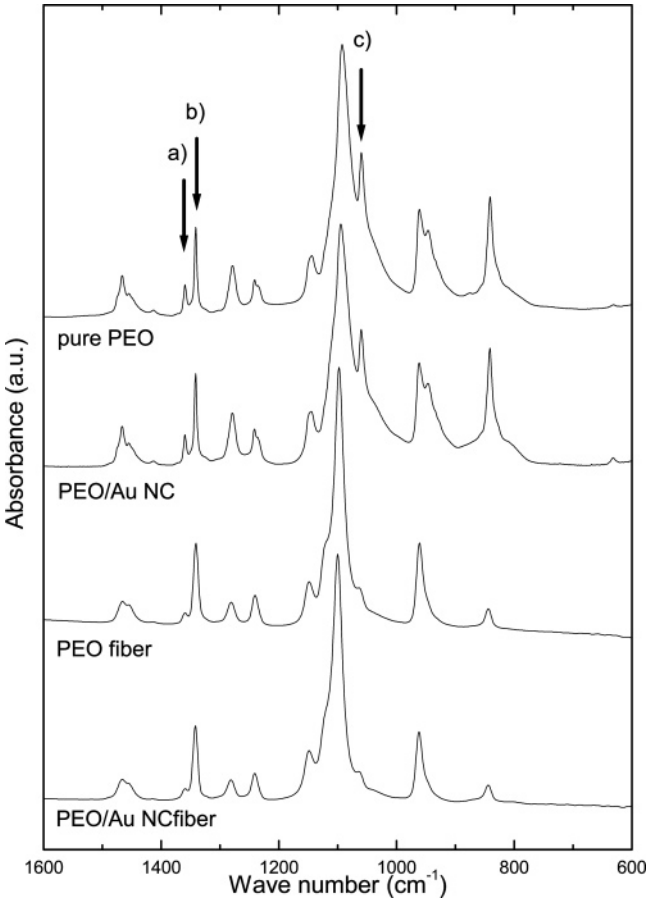

Figure 9. FTIR spectra for pure PEO, PEO/Au NC, electrospun PEO fibers, and PEO/Au NC fibers.

Table 3: FTIR Absorption Peaks for Amorphous (a) and Crystalline (x) PEO, Their Assignments, and Corresponding Dominant Conformational Types

absorption peak from a. PEO (cm^{-1})	absorption peak from x PEO (cm^{-1})	assignment	type of dominant conformation[a]
	1467	CH_2 bending	
1457			
	1455	CH_2 bending	
	1411	CH_2 wagging	
	1358	CH_2 wagging and CC stretching	H
1350			
	1341	CH_2 wagging	T
1292			
	1278	CH_2 twisting	H
1250			
	1240	CH_2 twisting	T
	1235	CH_2 twisting	H
	1144	CC stretching and COC stretching	
	1093	COC stretching	
	1060	CH_2 rocking and COC stretching	H
	961	CH_2 rocking	T
	947	CH_2 rocking	H
939			
850			
	842	CH_2 bending	H

[a] H and T are denoted by the helical and trans planar structure.

A_{1358}) increases after incorporation of Au nanoparticles and electrospinning, indicating an increase in the T population. The degree of the H-to-T conformational transformation of PEO upon incorporation of Au nanoparticles and electrospinning can be calculated as follows

$$HT\,(\%) = \left[\frac{(A_{1358}/A_{1341})_{\text{PEO/Au·NC·fiber·and·PEO·fiber}}}{(A_{1358}/A_{1341})_{\text{PEO}}} - 1\right] \times 100\%$$

As mentioned above, whereas an H band at 1060 cm^{-1} disappears after electrospinning of PEO (see arrow c in Figure 9), it can be clearly seen from Table 4 that the absolute T/H ratio of PEO/Au nanocomposite shifts to a higher value than that of electrospun PEO fibers without Au nanoparticles (twice in HT%). This means that Au nanoparticles preferentially induce the H-to-T conformational transformation, even more than electrospinning by itself. At the molecular level this may be associated with the fact that the dodecanethiol-capped Au nanoparticles interact with a sizable fraction of helical PEO chains, forcing them to become planar, thus favoring the conformational formation of T PEO.

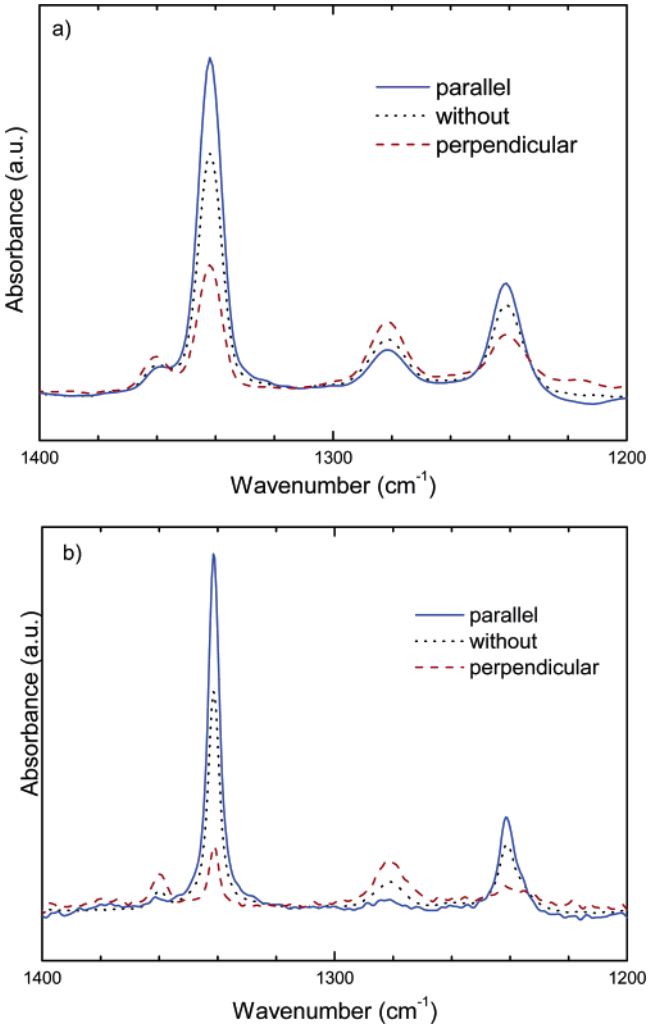

Figure 10. Polarized FTIR spectra for electrospun PEO fibers and PEO/Au NC fibers compared with spectra recorded without polarizing filter.

Table 4: Absorbance Peaks for Trans and Helix Conformation, Relative Population Ratios, and Fractions of the H-to-T Transformation

	T (A_{1341})	H (A_{1358})	T/H ratio	HT%
PEO	1429	1140	1.25	
PEO/Au NC	932	620	1.50	20
PEO fiber	696	508	1.37	10
PEO/Au NC fiber	1800	542	3.32	166

Due to the combination of Au nanoparticles with electrospinning, the electrospun PEO/Au fibers show the highest HT% of 170, which indicates that almost all PEO molecules in these fibers are in the trans state.[39]

To characterize the degree of molecular orientation of PEO within the electrospun fibers upon incorporation of Au nanoparticles, polarized FTIR measurements were performed. The results are shown in Figure 10, where the most characteristic T band at 1341 cm^{-1} was taken into consideration. Analysis was carried out by calculating the dichroic ratio, *R*, as the degree of molecule orientation, defined as follows

$$R = \frac{A_{1341\parallel}}{A_{1341\perp}}$$

where the subscripts $\parallel$ and $\perp$ denote parallel and perpendicular orientation relative to the fiber axis, respectively. The observed *R* values are 2.60 and 5.69 for the electrospun pure PEO fibers (Figure 10a) and PEO/Au NC fibers (Figure 10b), respectively. This indicates that the PEO molecules are more oriented parallel to the fiber axis in PEO/Au NC fibers than in pure PEO fibers, as expected according to the AFM results discussed before. As result, Au nanoparticles effectively facilitate the molecules aligning in the extensional flow direction during the electrospinning process.

(39) Bedrov, D.; Smith, G. D. *J. Chem. Phys*. **2003**, *118*, 6656.
(40) Known as the umbrella mode, which is essentially limited to the motion of the methyl group and therefore is relatively insensitive to the conformation of the rest of the chain. Hostetler, M. J.; Stokes, J. J.; Murray, R. W. *Langmuir* **1999**, *12*, 3604−3612.

4. Conclusions

In the present work the electrospinning process was successfully used to fabricate polymer nanofibers containing one-dimensional arrays of Au nanoparticles. The intrinsic nature of semicrystalline PEO was used as a template to arrange the Au nanoparticles within the fibers during electrospinning. TEM revealed that Au nanoparticles form quite long and one-dimensionally arranged chainlike arrays within the electrospun fibers. Thermal analysis and FTIR measurements showed that Au nanoparticles preferentially serve as nucleating sites during PEO crystallization and favor transforming the PEO molecular conformation from a helix to trans planar zigzag structure. The conformational transformation was dominantly affected by the presence of Au nanoparticles rather than by electrospinning itself. By means of combination of Au nanoparticles and electrospinning, the PEO molecules were preferentially aligned along the fiber axis, resulting in a perpendicularly arranged lamellar morphology, the so-called shish-kebab structure. Finally, the hybrid electrospinning shown in the present work provides great potential as a convenient and simple technique for the fabrication of one-dimensional arrays of metal nanoparticles suitable for processing into quantum-confined superstructures, in particular, future nanodevices. Their electrical and optical properties are currently under investigation.

Acknowledgment. The authors thank Dr. R. Adikari and Mr. M. Rosenthal for AFM investigation.

CM0508120